



Title	Signalling over a distance: gradient patterns and phosphorylation waves within single cells
Authors(s)	Muñoz-García, Javier, Kholodenko, Boris N.
Publication date	2010-10-01
Publication information	Muñoz-García, Javier, and Boris N. Kholodenko. "Signalling over a Distance: Gradient Patterns and Phosphorylation Waves within Single Cells." Portland Press, October 1, 2010. https://doi.org/10.1042/BST0381235 .
Publisher	Portland Press
Item record/more information	http://hdl.handle.net/10197/5578
Publisher's statement	The final version of record is available at http://dx.doi.org/10.1042/BST0381235 .
Publisher's version (DOI)	10.1042/BST0381235

Downloaded 2026-05-01 23:46:40

The UCD community has made this article openly available. Please share how this access benefits you. Your story matters! (@ucd_oa)



© Some rights reserved. For more information

Signalling over a distance: gradient patterns and phosphorylation waves within single cells

Javier Muñoz-García¹ and Boris N. Kholodenko^{1*}

¹Systems Biology Ireland, University College Dublin, Belfield, Dublin 4, Ireland

*Corresponding author: boris.kholodenko@ucd.ie

Abstract.

Recent discoveries of phosphorylation gradients and microdomains with different protein activities have revolutionised our perception of information transfer within single cells. The different spatial localization of opposing reactions in protein-modification cycles is shown to bring about heterogeneous stationary patterns and travelling waves of protein activities. We review spatial patterns and modes of signal transfer through phosphorylation/dephosphorylation and GDP/GTP exchange cycles and cascades. We show how switches between low-activity and high-activity states in a bistable activation-deactivation cycle can initiate the propagation of travelling protein-modification waves in the cytoplasm. Typically, an activation wave is initiated at the plasma membrane and propagates through the cytoplasm until it reaches the nucleus. An increase in deactivator activity is followed by the initiation of an inactivation wave that moves in the reverse direction from the nucleus. We show that the ratio of opposing enzyme rates is a key parameter that controls both the spread of activation through cascades and travelling waves.

Introduction

In the middle of the last century, seminal work of Alan Turing showed that biochemical reactions and diffusion can break the symmetry of initially homogeneous media and create periodic spatial patterns [1]. This work laid the foundation of the quantitative theory of morphogenesis [2]. Not surprisingly, the spatial dimension of signalling was subsequently analysed mainly in the context of morphogenesis and transmission of signals between cells. Single cells were viewed as well-stirred reaction vessels, uniformly stimulated by external cues. The advent of new imaging technologies and genetically encoded fluorescent biosensors has revolutionized our perception of the dynamic organization of signalling processes within single cells. Recent studies have revealed intricate spatial profiles of protein activities arising from signal-dependent formation of multi-protein complexes, their localization by anchoring subunits, dynamic self-assembly on scaffolds, and protein-lipid clustering [3-6]). This spatial heterogeneity is exploited to regulate key phenotypic cellular responses to external and internal cues. For instance, the mitotic spindle assembly is governed by the spatial gradients of RanGTP and other components of the chromosome-dependent RanGTPase-importin β cascade [7-9]. Cascades of small GTPases provide the spatial guidance and positional information related to cell motility, polarization, growth and differentiation [10, 11].

Cycles of reversible covalent modification of signalling proteins, catalyzed by opposing activator and deactivator enzymes, such as a kinase and phosphatase for a phospho-protein, or a guanine nucleotide exchange factor (GEF) and GTPase-activating protein (GAP) for small G-proteins form the backbones of cellular signal transduction pathways. The basic prerequisite for generation of signalling gradients by these cycles is the spatial segregation of the opposing enzymes that can localize to different cellular structures, such as membranes, chromosomes and cytoplasm. For instance, if a protein is phosphorylated by a membrane-bound kinase and dephosphorylated by a cytosolic phosphatase, a precipitous gradient of a phosphorylation form can occur, given measured values of protein diffusivity and typical kinase and phosphatase activities [12]. In protein interaction networks, the activity gradients are strongly controlled by the network design, including feedback and feedforward loops, and the cell shape and size [13-15].

Many key signal transmitters including activated protein kinases are stimulated at cell membranes and subsequently travel to distant sites in the cytoplasm or to the nucleus. However, the cytoplasmic localization of signal deactivators, such as phosphatases, can result in precipitous gradients of active, phosphorylated kinases and, therefore, low signal intensity at a distance from the membrane. This signal termination will hamper long-range signal transduction, especially in large cells, such as *Xenopus* oocytes or developing neurons [16, 17]. This puzzle has received much attention, and several mechanisms for long-range signal transduction within a cell, including endocytic trafficking [18], spatially distributed signalling cascades [19], retrograde transport in neurons, and travelling waves of protein phosphorylation have been proposed [16, 20, 21].

Cellular signalling networks are highly nonlinear and display intricate dynamics, including switch-like behaviour and bistability. Coexistence of two stable steady states and hysteresis are a hallmark of bistability [22, 23]. Coupled with diffusion, two stable states of biochemical systems create an active medium where signals can propagate by switching a system from an "off" state to an "on" state, or vice versa, creating trigger waves. Such propagating waves have been called travelling waves and studied earlier in the context of ecological and epidemiological models and

intracellular Ca signalling [24, 25]. Although this mechanism has been implicated in information transfer [16, 20, 26, 27], the conditions for signal propagation, attenuation, and reverse signal transmission have not been explored in the biochemical context. Here we review different modes of signal transfer within a cell. In particular, we analyze signal propagation by travelling waves that occur in bistable protein-modification cycles, such as activation-deactivation cycles of ERK, Src and small G-proteins [23, 28, 29]. We describe quantitative relationships that govern the direction of wave propagation and the reversal from activation travelling wave to inactivation wave.

Results.

Stationary activity gradients. One of simplest systems capable of generating stationary activity patters is a protein-modification cycle where an activating enzyme is localized to a membrane or cellular structure, whereas a deactivating enzyme is freely diffusible in the cytoplasm [12, 30-32]. Provided that the deactivator kinetics is far from saturation, the activated target concentration decays almost exponentially with the distance from the activating enzyme location (Fig. 1). The characteristic decay length of the gradient (L_{grad}) is controlled by the protein diffusivity (D) and the apparent first-order rate constant (k_{deact}) of the deactivating enzyme ($L_{grad} = \sqrt{D/k_{deact}}$), whereas this decay does not depend on the kinetics of the activating enzyme [12, 30, 31].

Spatial spread of activity gradients in linear cascades. For many signalling pathways, a plasma membrane receptor is stimulated by external cues and subsequently activates a cascade of protein-modification cycles that convey signals to nuclear targets [33]. Typically, the initiating kinase at the first cascade level is activated at the plasma membrane, as e.g., Raf-1 for the mitogen activated protein kinase (MAPK) cascade [34]. The activated form of the kinase, which diffuses inside the cell serves as an activating enzyme for the next cascade level and phosphorylates a downstream kinase (Fig. 2A). Although this mechanism can potentially spread the signal into the cell, activated kinases are dephosphorylated by cytoplasmic phosphatases, resulting in termination of the signal propagation [18]. Assuming that all kinases and phosphatases are far from saturation and the apparent first-order rate constants of kinases (k_{act}) and phosphatases (k_{deact}) are the same at the different cascade levels, their ratio $\gamma = k_{deact}/k_{act}$ is shown to be a key parameter that determines the spread of the activation signal [19]. When deactivation rates are too large, $\gamma > 1$, the propagation of signals stalls in the space, and the concentrations of activated kinases rapidly decay near the plasma membrane. If γ is sufficiently small, the signal carried by phosphorylated kinases spreads increasingly from the membrane towards the cell centre, generating spatial switches between almost complete dephosphorylated and phosphorylated forms (Fig. 2B). The spatial step size between consecutive decays of kinase activation for successive cascade layers is almost constant and equal to $\ln(1/\gamma)L_{grad}$ [19]. Thus, this landscape of consecutively decayed activities can serve as a precise spatial guidance for multiple cellular processes and convey information about the cell size to the nucleus.

Spatial dynamics of a bistable signalling cycle. We next consider a signalling molecule, such as a kinase or small GTPase, which is initially activated at the cell surface and then diffuses to the nucleus. We assume that in the cytoplasm, this molecule is autocatalytically activated. For instance, an inactive GDP-bound form of a small GTPase can initially be activated by a cell

membrane-bound GEF and then in the cytoplasm by another GEF, which often is autocatalytically activated by its product, an active GTPase form (Fig.3). Such autocatalytic activation was recently reported for the small GTPase Ras and its GEF SOS [35]. When RasGTP binds to the allosteric pocket of SOS, this causes a significant increase in SOS activity and, thus, further Ras activation [35]. Likewise, autocatalytic activation steps are also present in the activation-deactivation cycle of Src family kinases [28, 29]. An active form is deactivated in the cytoplasm by cytoplasmic enzymes, such as a phosphatase for kinases or GAP for small GTPases (Fig.3).

We analyse a one-dimensional geometry where the spatial coordinate, x , is confined by the plasma membrane (where the initial activation occurs) and the nuclear membrane, respectively. We do not consider the nuclear compartment and describe potential nuclear import, export and deactivation processes by a deactivation reaction at the nuclear membrane (Fig. 3). The temporal evolution of the active form concentration (C) is governed by the following reaction-diffusion equation [31],

$$\frac{\partial C}{\partial t} = D \frac{\partial^2 C}{\partial x^2} + v_a - v_d \quad (1)$$

Here v_a and v_d are the rates of activation and deactivation reactions in the cytoplasm. The diffusion constant D is assumed to be identical for both active and inactive (C_u) forms.

Therefore, the total protein concentration $C_{tot} = C + C_u$ does not depend on the spatial coordinate [6]. Assuming that both activator and deactivator enzymes in the cytoplasm follow Michaelis-Menten reaction mechanisms, their rate expressions can be presented as (see, e.g., [11]),

$$v_a = V_1 \frac{C_{tot} - C}{K_1 + (C_{tot} - C)} \cdot \frac{1 + AC/K_a}{1 + C/K_a}, \quad v_d = V_2 \frac{C}{K_2 + C}. \quad (2)$$

Here V_1 and V_2 are the maximal enzyme rates, K_1 , K_a and A are the Michaelis and activation constants. The boundary conditions to Eq. (1) equate the diffusive fluxes and the activation and deactivation rates at the cellular ($x=0$) and nuclear ($x=L$) membranes. For simplicity, we consider linear enzyme rates at both boundaries, but all results remain valid for the Michaelis-Menten expressions,

$$D \frac{\partial C}{\partial x} \Big|_{x=0,t} = -k_{PM} (C_{tot} - C|_{x=0,t}), \quad D \frac{\partial C}{\partial x} \Big|_{x=L,t} = k_{NM} C|_{x=L,t}, \quad (3)$$

where k_{PM} and k_{NM} are the surface reaction rate constants.

Since the ratio $\gamma \equiv V_1/V_2$ of the deactivator (V_2) and activator (V_1) rates is shown to be a critical system parameter [19], we first explore how the spatially homogeneous steady state(s) depend on this parameter. An enzyme cycle with autocatalytic steps can display bistability [31]. Indeed, for different γ values there are up to three steady states, which satisfy the steady-state condition ($v_a - v_d = 0$) that can be expressed, using the following dimensionless function ψ (Fig. 4),

$$\psi(C) \equiv (v_a - v_d)/V_1 = \frac{C_{tot} - C}{K_1 + (C_{tot} - C)} \cdot \frac{1 + AC/K_a}{1 + C/K_a} - \gamma \frac{C}{K_2 + C} = 0. \quad (4)$$

Within the bistability domain, the solution branches $C_1(\gamma)$ and $C_3(\gamma)$ are stable, while $C_2(\gamma)$ is the branch harbouring unstable states. The states $C_1(\gamma)$ and $C_3(\gamma)$ are referred to as high- and low-activity states, respectively.

Activation and deactivation waves. Reaction-diffusion equations, such as Eq.1, that display bistable reaction dynamics may have travelling wave solutions [24]. These solutions describe the propagation of a reaction front that switches the system from one stable state to the other stable state over a space region. This is an efficient mechanism for the propagation of intracellular signals over large distances with a constant speed, significantly faster than simple diffusion [26].

On an infinite spatial domain, the travelling wave front that connects two alternative, stable steady states moves with a constant speed (s) without changing the shape. To describe the front profile, we consider a co-moving reference frame by introducing the new variable, $z \equiv x - st$. Within this moving frame, the wave shape does not change and can be described as a function of only this variable, $U(z) \equiv C(x, t)$. The value $z=0$ corresponds to an arbitrary chosen point, for instance, where the active form concentration equals $(C_1+C_3)/2$. After substitution $U(z)$, into Eq.1, we obtain,

$$D \frac{d^2U}{dz^2} + s \frac{dU}{dz} + v_a(U) - v_d(U) = 0. \quad (5)$$

Typical boundary conditions assume that at one end (e.g., the rear wave end), the system is at the high-activity steady state $U(z \rightarrow -\infty) = C_3$, whereas at the other end, the system is at low-activity state $U(z \rightarrow \infty) = C_1$. In biological terms, these conditions imply that at the plasma membrane the system is at the high-activity state, whereas at the nuclear membrane it remains at low-activity state. If the wave travels in the positive direction (from the plasma membrane to the nucleus), the system switches from the low- to high-activity state in the cytoplasm, and vice versa.

Supplement 1 shows that the sign of the propagation velocity that determines the direction of the wave is given by the sign of the following integral [24, 27],

$$I(\gamma) \equiv \int_{C_1}^{C_3} \psi(C) dC. \quad (6)$$

Depending on the ratio $\gamma = V_1/V_2$ of the deactivating and activating rates, the sign of the integral $I(\gamma)$ can be negative or positive (Fig. 4A). For positive values of this integral, the speed s is positive, and the wave moves towards increasing x values. Then, the high-activity state C_3 gradually invades the whole spatial domain, advancing with a constant speed (Fig. 5A). On the other hand, if this integral is negative, the low-activity state C_1 becomes dominant. This corresponds to an inactivation wave that moves backward from the nucleus to the plasma membrane (Fig. 5B). Thus, changing the activity ratio γ provides a way to control activation and consecutive inactivation of signalling by changing the catalytic rates or expression levels of activator and deactivator enzymes. Fig. 5A illustrates how activation wave is initiated at the plasma membrane and propagates through the cytoplasm until it reaches the nucleus. This is followed by an inactivation wave moving in the reverse direction after an increase in deactivator activity (Fig. 5B, V_2 increased). Note, that changing γ also modifies the active form concentration corresponding to spatially homogeneous steady states. Although the new value of C_1 remains almost identical to the old one, the active form concentration at the state C_3 is lower for inactivation wave than for activation wave (see also Fig. 4).

Travelling phosphorylation waves in protein kinase cascades. We and other groups have recently shown that bistability is a fundamental feature of the control of protein activity by multisite covalent modification and the extracellular regulated kinase (ERK) activation-

deactivation cycle itself can exhibit bistability [23, 36-38]. Analysis of the spatio-temporal dynamics showed that bistability in the ERK cycle can give rise to trigger waves that propagate binary phosphorylation signals from the plasma membrane receptors to distant targets [26]. If a downstream kinase, such as ERK, stimulates the activation of the upstream kinase (directly or via a regulatory circuit in the cytoplasm), a resulting bistable switch generates a traveling cytoplasmic wave that propagates over increasingly long distances with nearly constant amplitude and velocity [26]. These traveling waves of protein phosphorylation present a novel mechanism of long-range signaling within cells, when phosphorylation signals cannot be transferred by diffusion.

Concluding remarks

Recent evidence suggests that signalling protein activities are remarkably heterogenous within cellular space. Subcellular domains of different protein activities can arise solely from the dynamics of chemical transformations coupled with diffusion. For instance, Turing's patterns are driven by the instability of a spatially uniform distribution of two species, commonly termed activator and inhibitor, which have different diffusion coefficients (diffusivities), and the activator autocatalytically reproduces itself and stimulates its inhibitor [1, 2]. Another biochemical mechanism that generates stable, stationary patterns of concentration and activity gradients exploits the pre-existing structural heterogeneity [12, 19]. Due to the cell heterogeneity, many signalling proteins are spatially separated, for instance some proteins are bound to membranes, whereas the other retain in the cytoplasm, or shuttle between the cytoplasm and the nucleus.

Intricate temporal dynamics of signalling systems lead to complex spatial phenomena, including cell polarization, pattern formation and travelling waves. Here we show that bistable switches in an autocatalytic protein-modification cycle (Fig. 3) may result in both activation and deactivation waves propagating through single cells (Fig. 5). For different rates of the opposing activator and deactivator enzymes only activating waves (switching the system globally into the "ON" state) or only deactivating waves (switching the system into the "OFF" state) can exist. The regulation of the activation and deactivation enzyme activities provides a mechanism of precise control over global activation and deactivation waves.

Acknowledgement. Supported by Science Foundation Ireland under Grant No. 06/CE/B1129 and NIH grant GM059570. BNK is a SFI Stokes Professor of Systems Biology.

References

- 1 Turing, A. M. (1952) The chemical basis of morphogenesis. *Phil. Trans. R. Soc. Lond. B Biol Sci.* **237**, 37-72
- 2 Gierer, A. (1981) Generation of biological patterns and form: some physical, mathematical, and logical aspects. *Prog Biophys Mol Biol.* **37**, 1-47
- 3 Suzuki, K. G., Fujiwara, T. K., Sanematsu, F., Iino, R., Edidin, M. and Kusumi, A. (2007) GPI-anchored receptor clusters transiently recruit Lyn and G alpha for temporary cluster immobilization and Lyn activation: single-molecule tracking study 1. *J Cell Biol.* **177**, 717-730
- 4 Inder, K., Harding, A., Plowman, S. J., Philips, M. R., Parton, R. G. and Hancock, J. F. (2008) Activation of the MAPK module from different spatial locations generates distinct system outputs. *Mol Biol Cell.* **19**, 4776-84
- 5 Shapiro, L., McAdams, H. H. and Losick, R. (2009) Why and how bacteria localize proteins. *Science.* **326**, 1225-1228
- 6 Kholodenko, B. N. (2009) Spatially distributed cell signalling. *FEBS Lett.* **583**, 4006-4012
- 7 Kalab, P., Weis, K. and Heald, R. (2002) Visualization of a Ran-GTP gradient in interphase and mitotic *Xenopus* egg extracts, *Science.* **295**, 2452-2456
- 8 Caudron, M., Bunt, G., Bastiaens, P. and Karsenti, E. (2005) Spatial coordination of spindle assembly by chromosome-mediated signaling gradients. *Science.* **309**, 1373-1376
- 9 Athale, C. A., Dinarina, A., Mora-Coral, M., Pugieux, C., Nedelec, F. and Karsenti, E. (2008) Regulation of microtubule dynamics by reaction cascades around chromosomes. *Science.* **322**, 1243-1247.
- 10 Dawes, A. T. and Edelstein-Keshet, L. (2007) Phosphoinositides and Rho proteins spatially regulate actin polymerization to initiate and maintain directed movement in a one-dimensional model of a motile cell. *Biophys J.* **92**, 744-768
- 11 Stelling, J. and Kholodenko, B. N. (2008) Signaling cascades as cellular devices for spatial computations. *J Math Biol.* **58**, 35-55
- 12 Brown, G. C. and Kholodenko, B. N. (1999) Spatial gradients of cellular phospho-proteins. *FEBS Lett.* **457**, 452-454.
- 13 Meyers, J., Craig, J. and Odde, D. J. (2006) Potential for Control of Signaling Pathways via Cell Size and Shape. *Curr Biol.* **16**, 1685-1693
- 14 Neves, S. R., Tsokas, P., Sarkar, A., Grace, E. A., Rangamani, P., Taubenfeld, S. M., Alberini, C. M., Schaff, J. C., Blitzler, R. D., Moraru, II and Iyengar, R. (2008) Cell shape and negative links in regulatory motifs together control spatial information flow in signaling networks. *Cell.* **133**, 666-680
- 15 Kholodenko, B. N. and Kolch, W. (2008) Giving space to cell signaling. *Cell.* **133**, 566-567
- 16 Kholodenko, B. N. (2003) Four-dimensional organization of protein kinase signaling cascades: the roles of diffusion, endocytosis and molecular motors. *J Exp Biol.* **206**, 2073-2082
- 17 Rishal, I. and Fainzilber, M. (2009) Retrograde signaling in axonal regeneration. *Exp Neurol.*
- 18 Kholodenko, B. N. (2002) MAP kinase cascade signaling and endocytic trafficking: a marriage of convenience? *Trends Cell Biol.* **12**, 173-177
- 19 Muñoz-García, J., Neufeld, Z. and Kholodenko, B. N. (2009) Positional information generated by spatially distributed signaling cascades. *PLoS Comput Biol.* **5**, e1000330
- 20 Reynolds, A. R., Tischer, C., Verveer, P. J., Rocks, O. and Bastiaens, P. I. (2003) EGFR activation coupled to inhibition of tyrosine phosphatases causes lateral signal propagation. *Nat Cell Biol.* **5**, 447-453

- 21 Perlson, E., Michaelevski, I., Kowalsman, N., Ben-Yaakov, K., Shaked, M., Seger, R., Eisenstein, M. and Fainzilber, M. (2006) Vimentin binding to phosphorylated Erk sterically hinders enzymatic dephosphorylation of the kinase. *J Mol Biol.* **364**, 938-944
- 22 Ferrell, J. E., Jr. (2002) Self-perpetuating states in signal transduction: positive feedback, double-negative feedback and bistability. *Curr Opin Cell Biol.* **14**, 140-148
- 23 Markevich, N. I., Hoek, J. B. and Kholodenko, B. N. (2004) Signaling switches and bistability arising from multisite phosphorylation in protein kinase cascades. *J Cell Biol.* **164**, 353-359
- 24 Murray, J. D. (2001) *Mathematical Biology*, Springer, New York
- 25 Keener, J. and Sneyd, J. (1998) *Mathematical Physiology*, Springer, New York
- 26 Markevich, N. I., Tsyganov, M. A., Hoek, J. B. and Kholodenko, B. N. (2006) Long-range signaling by phosphoprotein waves arising from bistability in protein kinase cascades. *Mol Syst Biol.* **2**, 61
- 27 Mori, Y., Jilkine, A. and Edelstein-Keshet, L. (2008) Wave-pinning and cell polarity from a bistable reaction-diffusion system. *Biophys J.* **94**, 3684-3697
- 28 Fuss, H., Dubitzky, W., Downes, S. and Kurth, M. J. (2006) Bistable switching and excitable behaviour in the activation of Src at mitosis. *Bioinformatics.* **22**, e158-165
- 29 Kaimachnikov, N. P. and Kholodenko, B. N. (2009) Toggle switches, pulses and oscillations are intrinsic properties of the Src activation/deactivation cycle. *Febs J.* **276**, 4102-4118
- 30 Freedman, T. S., Sondermann, H., Friedland, G. D., Kortemme, T., Bar-Sagi, D., Marqusee, S. and Kuriyan, J. (2006) A Ras-induced conformational switch in the Ras activator Son of sevenless. *Proc Natl Acad Sci U S A.* **103**, 16692-16697
- 31 Kholodenko, B. N. (2006) Cell-signalling dynamics in time and space. *Nat Rev Mol Cell Biol.* **7**, 165-176
- 32 Maeder, C. I., Hink, M. A., Kinkhabwala, A., Mayr, R., Bastiaens, P. I. and Knop, M. (2007) Spatial regulation of Fus3 MAP kinase activity through a reaction-diffusion mechanism in yeast pheromone signalling. *Nat Cell Biol.* **9**, 1319-1326
33. Borisov, N., Aksamitiene, E., Kiyatkin, A., Legewie, S., Berkhout, J., Maiwald, T., Kaimachnikov, N. P., Timmer, J., Hoek, J. B. and Kholodenko, B. N. (2009) Systems-level interactions between insulin-EGF networks amplify mitogenic signaling. *Mol Syst Biol.* **5**, 256
34. Kolch, W. (2000) Meaningful relationships: the regulation of the Ras/Raf/MEK/ERK pathway by protein interactions. *Biochem J.* **351** Pt 2, 289-305
35. Freedman, T. S., Sondermann, H., Friedland, G. D., Kortemme, T., Bar-Sagi, D., Marqusee, S. and Kuriyan, J. (2006) A Ras-induced conformational switch in the Ras activator Son of sevenless. *Proc Natl Acad Sci U S A.* **103**, 16692-16697
36. Harding, A., Tian, T., Westbury, E., Frische, E. and Hancock, J. F. (2005) Subcellular localization determines MAP kinase signal output. *Curr Biol.* **15**, 869-873
37. Ortega, F., Garces, J. L., Mas, F., Kholodenko, B. N. and Cascante, M. (2006) Bistability from double phosphorylation in signal transduction. *Febs J.* **273**, 3915-3926
38. Wang, X., Hao, N., Dohlman, H. G. and Elston, T. C. (2006) Bistability, stochasticity, and oscillations in the mitogen-activated protein kinase cascade. *Biophys J.* **90**, 1961-1978

Figure legends

Fig. 1: Gradient of spatial activity in a single protein-modification cycle. (A) Sketch of a protein-modification cycle, in which an inactive form (C_u) is activated at the plasma membrane, yielding an active form (C). Both forms, C and C_u diffuse in the cytoplasm, where C is deactivated by cytoplasmic enzymes. (B) Spatial decay of C as a function of the distance from the plasma membrane, $D = 1 \mu\text{m}^2/\text{s}$, $k_{deact} = 0.16 \text{ s}^{-1}$, $L_{grad} = (D/k_{deact})^{1/2} = 2.5 \mu\text{m}$.

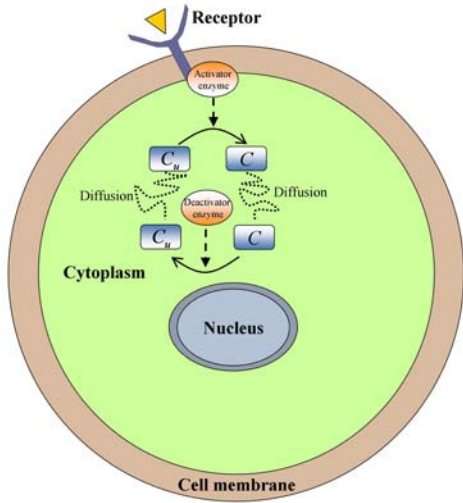
Fig. 2: Spatial propagation of activated forms for a cascade of protein-modification cycles. (A) Cascade diagram. At the first level, an inactive form C_u^1 is activated at the plasma membrane, yielding an active form C^1 . Each active form C^i at level $i = 1, 2, \dots, N-1$ catalyzes activation of the downstream inactive form C_u^{i+1} and is deactivated by cytoplasmic enzymes. (B) Stationary spatial patterns formed by consecutive active forms for a 5-tier cascade, $D = 1 \mu\text{m}^2/\text{s}$, $\gamma = k_{deact}/k_{act} = 0.05$.

Fig. 3: Sketch of a reaction scheme for a bistable autocatalytic cycle. An inactive protein form (C_u) is initially activated at the plasma membrane. Both forms, C and C_u diffuse in the cytoplasm where C_u is autocatalytically activated and C is deactivated by cytoplasmic enzymes.

Fig. 4. Uniform stationary concentrations of active form C of a target protein. (A) The dimensionless function ψ (which is the difference between the activation and inactivation rates normalized by V_1) is plotted as a function of C for different values of $\gamma = 14, 16, 18,$ and 20 from top to bottom. Uniform steady state solutions are given by intersections with the zero axis, $\psi(C) = 0$. (B) Dependence of the uniform steady-state solutions on γ . Solid and dashed lines represent stable (C_1 and C_3) and unstable (C_2) solution branches, respectively. The parameter values are $C_{tot} = 150 \text{ nM}$, $K_I = 50 \text{ nM}$, $K_2 = 2.5 \text{ nM}$, $K_a = 50 \text{ nM}$, and $A = 50$.

Fig. 5. Temporal evolution of the concentration profiles for activation and deactivation travelling waves. The dependence of active form concentration C on space and time is obtained by numerical integration of Eq.1. The parameter values are given in Fig.2, $D = 1 \mu\text{m}^2/\text{s}$, $V_I = 10 \text{ nM/s}$, $k_{PM} = k_{NM} = 0.5 \mu\text{m/s}$, and $L = 25 \text{ nm}$. (A) $V_2 = 140 \text{ nM/s}$; $t = 10, 20, 30, 40,$ and 60 s (profiles from left to right). (B) At $t = 60 \text{ s}$ the deactivator activity is increased to $V_2 = 180 \text{ nM/s}$; $t = 80, 90, 100, 110,$ and 120 s (profiles from right to left).

(A)



(B)

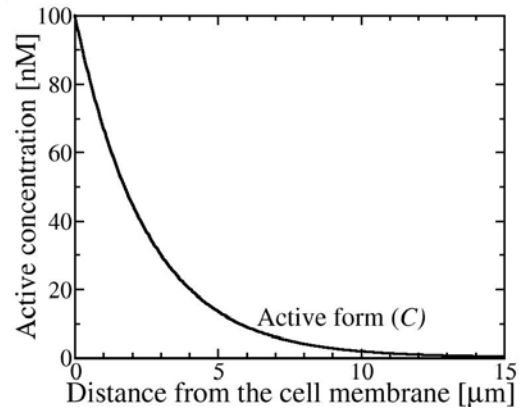
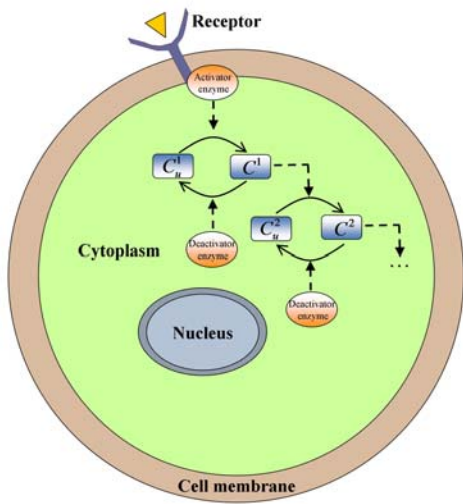


Fig. 1

(A)



(B)

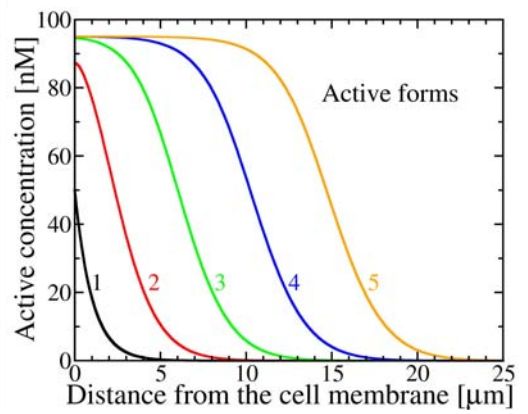


Fig. 2

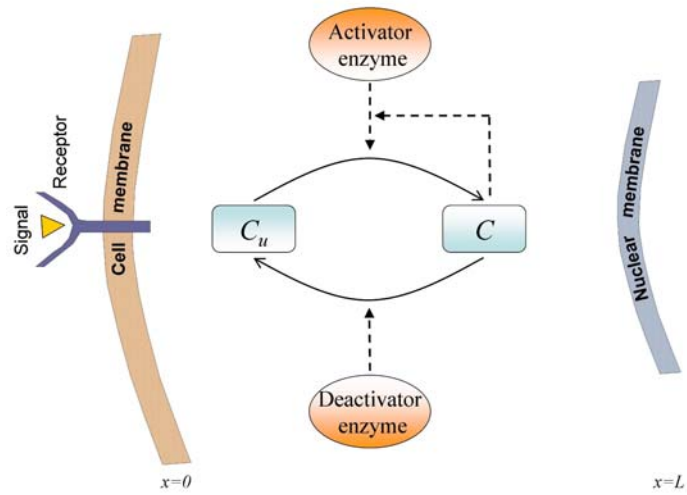


Fig. 3

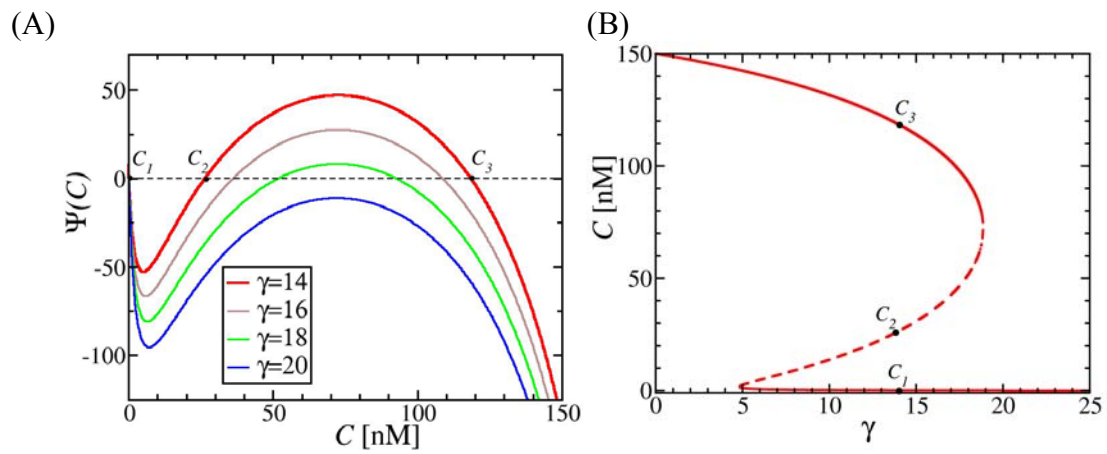


Fig. 4

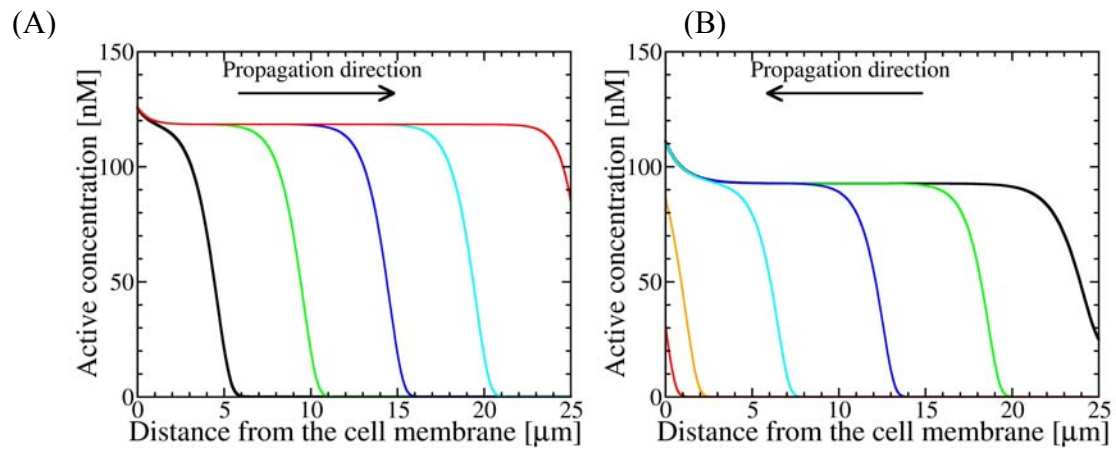


Fig. 5

Signalling over a distance: gradient patterns and phosphorylation waves within single cells.

Supplementary material.

Javier Muñoz-García¹ and Boris N. Kholodenko^{1*}

Supplement 1.

The sign of the wave velocity, and hence the direction of the propagation, can be found by multiplying Eq.5 by dU / dz and integrating from $z \rightarrow -\infty$ to $z \rightarrow \infty$. This leads to the following,

$$\int_{-\infty}^{\infty} \left\{ D \frac{d^2 U}{dz^2} \frac{dU}{dz} + s \left(\frac{dU}{dz} \right)^2 + [v_a(U) - v_d(U)] \frac{dU}{dz} \right\} dz = 0. \quad (\text{S1.1})$$

Assuming that the solution U is uniform far from the travelling front (i.e. $dU / dz(z \rightarrow \pm\infty) = 0$), the first term in (S1.1) vanishes. Since $U(z \rightarrow -\infty) = C_3$, and $U(z \rightarrow \infty) = C_1$, we obtain,

$$s \int_{-\infty}^{\infty} \left(\frac{dU}{dz} \right)^2 dz = - \int_{-\infty}^{\infty} [v_a(U) - v_d(U)] \frac{dU}{dz} dz = - \int_{C_3}^{C_1} [v_a(C) - v_d(C)] dC. \quad (\text{S1.2})$$

Here the right hand side of (S1.2) was integrated by parts and expressed in terms of the original variable C . Dividing by V_1 and reversing limits of integration on the right hand side of (S1.2) we obtain

$$s = \frac{V_1 \int_{C_3}^{C_1} \Psi(C) dC}{\int_{-\infty}^{\infty} \left(\frac{dU}{dz} \right)^2 dz}. \quad (\text{S1.3})$$

Equation (S1.3) shows that the sign of s only depends on the sign of the definite integral of ψ between the two stationary stable states, see Eq.6 of the main text. Another interesting ramification of Eq. S1.3 is that the wave velocity scales with the value of V_1 (at constant γ).